A DFT and SERS Study of Synergistic Roles of Thermodynamics and Kinetics During the Electrocatalytic Reduction of Benzyl Chloride at Silver Cathodes

Yan-Li Chen,[a,b] Ting-Wei Weng,[a] Zhuan-Yun Cai,[a] Hang Shi,[a] Tai-Rui Wu,[a] De-Yin Wu,*[a,d] Alexander Oleinick,[c,d] Irina Svir,[c,d] Bing-Wei Mao,[a,d] Christian Amatore,*[a,c,d] and Zhong-Qun Tian*[a,d]

a State Key Laboratory of Physical Chemistry of Solid Surfaces and Department of Chemistry, College of Chemistry and Chemical Engineering, Xiamen University, Xiamen 361005, China

b Jiangsu Key Laboratory of Advanced Catalytic Materials and Technology, School of Petrochemical Engineering, Changzhou University, Changzhou 213164, China.

c PASTEUR, Département de Chimie, École Normale Supérieure, PSL University, Sorbonne Université, CNRS, 24 rue Lhomond, 75005 Paris, France.

d Sino-French CNRS IRP NanoBioCatEchem International Laboratory.

E-mails: <dywu@xmu.edu.cn>;<christian.amatore@ens.psl.eu>;<zqtian@xmu.edu.cn>

(Dedicated to Professor Shaojun Dong for her 90th Birthday)

Abstract

The reductive cleavage of carbon-halogen bonds is one of the classical model systems of concerted versus non-concerted bond breaking electron transfer in molecular electrochemistry, but most studies did not consider the influence of adsorption of reaction intermediates on this phenomenon. We performed density functional theory (DFT) calculations to understand the electrochemical reduction of benzyl chloride at silver electrodes through predicting the surface adsorption effect of the reactant and of follow-up intermediates and analyzing the energetics of the overall dissociative electron transfer. The ensuing DFT calculations of surface-enhanced Raman spectroscopic (SERS) signals provided some key information for characterizing different surface species at different potentials at the molecular level. The most intense and broad spectral peak observed near 800 cm^{-1} in the electrochemical SERS was thus assigned to the CH_2 wagging vibration closely associated with the co-adsorption of benzyl radical and chlorine. After the dissociation of the C-Cl benzyl chloride bond, the chloride anion adsorbs at the three-fold hollow site on silver electrodes, as indicated by a low vibrational frequency and a weak Raman signal. Conversely, the formed benzyl radical intermediate is found to adsorb at the top site with the characteristic vibrational frequency and strong Raman intensity. DFT calculations further confirmed that the kinetic effect underlying the electrocatalytic activity of silver electrodes is closely associated with the intrinsic energy barrier and the dissociative adsorption state of benzyl radical and chlorine on silver electrodes. Finally, we discuss the fundamental meaning of the kinetic rate constant of

the first-step dissociative electron transfer for benzyl chloride on silver electrodes based on the different electron transfer models, indicating the synergistic roles of thermodynamics and kinetics.

Keywords: Benzyl Chloride; Silver Electrode; Bond Dissociative Electron Transfer; Density Functional Theory; Surface-Enhanced Raman spectroscopy

Introduction

Electrochemical activation of carbon-halogen bonds has always been a central issue in molecular electrochemistry. Recently, there is a renewed and growing interest in achieving a fine understanding of these processes. They play indeed a significant role not only in synthetic chemistry or for possible storage of volatile electrical energy through electrosynthesis, but also environmental science. For example, electrochemical reduction of pesticide residues containing carbon-halogen bonds allows their removal from environment, so as to improve human health and food safety.[1, 2] On another and more fundamental electrochemical grounds, the reductive cleavage of carbon-halogen bonds has rapidly established itself as the model system of concerted or non-concerted bond breaking electron transfer.[3-5] There are indeed two main possible pathways to reductively cleave carbon-halogen bonds. In the earliest proposed mechanisms, the cleavage was supposed to occur sequentially through the initial formation of the organic-halide anion radical that was then undergoing a carbon-halogen bond-breaking reaction. Several mechanistic clues hinted that this formerly widely accepted mechanism could not account for some kinetic observations. Saveant and his coworkers introduced the notion of concerted mechanisms, in which the initial one-electron uptake by parent organic halide directly produces a radical and a halide ion without any intermediate anion radical which they established on glassy carbon electrodes.[3, 5, 6] Prior to Saveant's contributions this was supposed to occur for organic halides in which the carbon-halogen σ^* orbital or a larger molecular orbital involving the σ^* orbital is the only available orbital prone to accept an electron as in some aromatic-halides. Indeed, the sequential vs concerted pathway depends on the importance of coupling between the organic π^* and carbon-halogen σ^* orbitals. In any case, the σ-radicals formed after the concerted or non-concerted cleavage have generally reduction potentials that are largely positive to the reduction potential of the parent organic halide, so that they are immediately reduced into the corresponding organic anion moiety when the overall mechanistic sequence occurs at the outer Helmholtz plane (OHP) or farther in solution, *i.e.*, without any involvement of the electrode surface, as occurs at glassy carbon and mercury electrodes.[3]

However, electrode materials and solvent as well as electrode potentials have been observed to play a significant role which has added to the complexity of mechanistic problems at hand, especially when no clear evidence of adsorption of reactants and intermediates could be obtained.[7-11] In recent years, it has been found that coinage metals (e.g., Ag, Cu, Pd and

Ni) possesses high catalytic activity for the reduction of several organic halides. Among them, silver was shown to exhibit surprisingly high electrocatalytic property.[7-12] For example, the irreversible voltammetric reduction wave of the benzyl chloride at silver cathodes was found to shift positively by at least 0.5 V with respect to that at glassy carbon electrodes which are usually regarded as a reference model for inert electrodes. Such a phenomenon has motivated a widespread interest, and the search for the exact reasons that sustain such exceptional electrocatalytic effect has rapidly focused on the reduction of benzyl chloride at silver cathodes taken as a model system.[7, 10, 13-15] However, due to the lack of precise means for characterizing and investigating the existence of any interfacial metal-substrate or metal-intermediate structures, the problem has long remained unsolved or speculative. For example, based on a series of carefully planned works it has been suggested that a strong adsorption of the halogen of the parent substrate prior to the first electron uptake,[7] or of the halide anion during/after reduction could play a particularly crucial role,[10] although Cl^- had been previously reported to desorb over the potential range in which the benzyl chloride reduction occurs. Clearly, despite the strong efforts aimed to solve this puzzle, no convincing solution could be brought in the absence of any information possibly gathered at the molecular level through precise dynamic investigations of the silver interface during the electrochemical reaction.

Surface-enhanced Raman spectroscopy (SERS), a spectroscopic methodology with high detection sensitivity, high spatial resolution, and high energy resolution has established itself as an important tool for the study of electrochemical interfaces at the molecular level through allowing a precise characterization of adsorbed molecules structures. These unique SERS characteristics were recently extended to provide exceptional information about reaction processes undergoing at electrode surfaces during complex electrochemical reactions.[16-18] For this reason, several of us decided to rely on SERS to monitor the electrochemical reduction of benzyl chloride at a silver electrode in acetonitrile solution, and found that although at usual scan rates the irreversible voltammetric wave of benzyl chloride reduction at silver electrodes exhibits typical mechanistic characteristics hinting to a process occurring in solution, the potential range over which it is displayed could be divided into three main regions based on SERS evidences. Distinct SERS spectra characterizing different surface species were recorded during the reduction of $PhCH_2Cl$ at a Ag electrode in acetonitrile, depending on the potential domain, namely, [-0.9 ~ -1.2 V] (**I**), [-1.2 ~ -1.8 V] (**II**), and [-1.8 ~ -2.2 V] (**III**) vs. saturated calomel electrode (SCE),. These corresponded respectively to weakly adsorbed benzyl chloride (**I**), strongly adsorbed reaction intermediates (**II**) and reaction products (**III**).[11, 19-21] Based on DFT calculations, the strongest SERS peak observed in the region (**II**) could be ascribed to the out-of-plane wagging bending vibration of the methylene (CH_2) group pertaining to the benzyl radical/anion species adsorbed on the silver surface, *i.e.*, $PhCH_2^{\bullet}$ or $PhCH_2^-$, the intermediates generated after the first and the second electron uptake, respectively.[19] These results suggested that $PhCH_2^{\bullet}$/$PhCH_2^-$ moieties should be adsorbed through their methylene carbon onto the Ag electrode surface. Both intermediates displayed strong adsorption interaction with the Ag electrode surface, as evidenced by the fact that the Raman spectra of their adsorption states were significantly different from those predicted for free benzyl radical and its anions.[19, 22, 23] Although this could not be ascertained in those previous investigations, the fate of the adsorbed $PhCH_2^{\bullet}$ is

presumably dependent on the electrode surface charge. When the electrode potential is more positive than the potential of zero charge (PZC), the adsorption should stabilize the radical and increase its surface concentration contributing to yield its coupling instead of its reduction. [8, 14] Conversely, at potentials more negative than the PZC, as certainly happens during the reduction of benzyl chloride, benzyl radicals are expected to be easily reducible into benzyl anions which may then be mostly protonated to yield the relevant hydrocarbon. These views agreed with the fact that the reduction of benzyl chloride at the Ag electrode produced mainly toluene ($PhCH_3$), which is also the main product at glassy carbon electrodes,[9] 1,2-diphenylethane ($PhCH_2CH_2Ph$), although in minute quantities, and 3-hydrocinnamonitrile ($PhCH_2CH_2CN$) which probably resulted from a coupling of the benzyl radical with the $^{\bullet}CH_2CN$ radical formed by H-atom abstraction from the solvent. [24]

Therefore, our former series of works[19-23] based on a coupling of voltammetric, SERS and DFT results considerably clarified the question. However, due to the limitation of the system sizes that could be investigated by DFT at the time, these theoretical approaches had to be limited to small Ag_n clusters to model the silver cathode surfaces. This prevented examining the role and effect of any synergetic interactions due, for example, to a transient halogen anion adsorption together with that of the benzyl radical. We wish therefore to present now a more detailed investigation of the structures and energies of adsorbed species on silver surface modeled by different Ag_n clusters (n = 3, 4, 5, 6, 13, 19) including benzyl chloride, its activated complex during the concerted reduction, without neglecting the role of possible other co-adsorbed species such as Cl-based species. This allowed a better description of the electrocatalytic mechanism occurring at silver cathodes.

Computational Methods and Details

Charged metal cluster models were used to investigate theoretically the adsorption site on the silver electrode surface. Here we adopted different size Ag clusters Ag_n (n = 3, 4, 5, 6, 13, 19) to simulate the adsorption site on the silver electrode surface. Figure 1 presents the structure of free benzyl chloride, adsorbed benzyl chloride and its dissociative products on Ag_{19} clusters. The Ag_{19} cluster used here is quite suitable to describe the defect site with one negative charge which will be localized at the adsorption site. Optimized structures of other molecule-cluster complexes are also provided in following sections. As expected, in the free benzyl chloride molecule, the carbon-chlorine bond resting in the plane perpendicular to the benzene ring and being oriented towards the silver surface corresponded to the structure of lowest energy (Figure 1b). For the adsorption of benzyl chloride on the silver surface, three kinds of configurations were envisioned for the binding of the chlorine atom to the Ag clusters, that is, involving top, bridge or hollow sites. However, after DFT geometry optimization, the chlorine atom of undissociated benzyl chloride tended to always adsorb at the top site. A total of 3 optimized adsorption structures (Figure 1c-e) were thus obtained for benzyl chloride binding to Ag_{19} before its reduction, with that in Figure 1c being the most stable one. When keeping an overall zero charge for the molecule-cluster complexes, the benzyl chloride moiety was observed to spontaneously dissociate into a chloride ion adsorbed at the hollow site and a benzyl radical adsorbed at the top site, as shown in Figure 1f-g. However, Figure 1h illustrates that a different situation in which the benzyl radical directly interacted with the chloride ion adsorbed at the hollow site could be obtained.

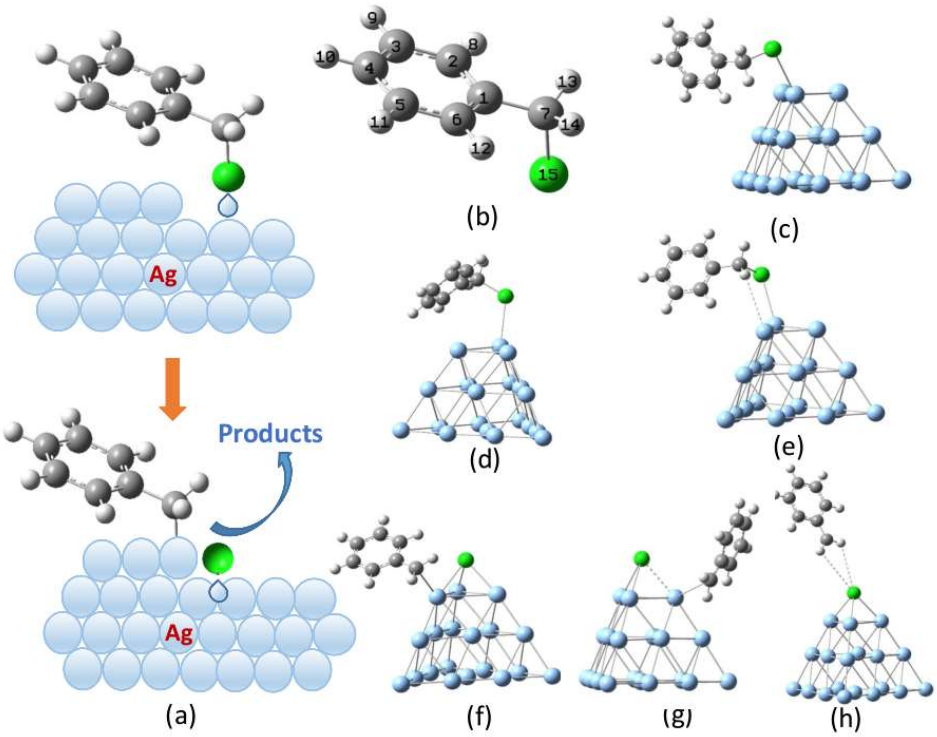

Figure 1. Left: (a) schematic representation of $PhCH_2Cl$ adsorption followed by a dissociative electron transfer. Right (b-h): optimized DFT structures of (b) pristine benzyl chloride; (c, d, e) adsorption configurations of non-dissociated benzyl chloride onto the Ag_{19} cluster complexes; (f, g, h) adsorption configurations after dissociation where the chlorine atom always locates at the hollow site while the benzyl moiety adsorbs either directly onto an adjacent Ag top site (f,g) or through a mediated interaction by the Cl moiety (h). Although the solvent contributions are not shown they were taken into account through using the polarizable continuum model. [25]

For the above molecule-metal complexes, hybrid exchange-correlation functional B3LYP approaches [26] were adopted to perform full geometric optimization of structures and energy calculations. For C, Cl, and H atoms, all electrons were described by adopting full-electron basis sets 6-311+G**[27] or the Dunning basis set[28], respectively. Both polarization and diffuse functions were used for C and Cl atoms, whereas only polarization function was used for H atoms. For Ag atoms, the small core pseudo-potential basis set LANL2DZ was adopted. [29] The twenty-eight electrons of Ag atoms in the inner shells were described by the pseudo-potential method, while 19 electrons in the valence shell $4s^2 4p^6 4d^{10} 5s^1$ were described by double-ζ basis. To include the organic solvent effect, we employed the polarizable continuum model (PCM), [25] using a static dielectric constant 35.688 for acetonitrile. The thermodynamic energies presented thereafter are referred to one standard atmosphere and 298.15K. [30] The energies of benzyl chloride, benzyl radical, and silver clusters were used to calculate the negative binding energies. The adsorption energy ΔE and Gibbs free energy ΔG of benzyl species interacting with silver clusters were calculated as:

$$\Delta E = E_{Mol-Ag_n} - E_{Ag_n} - E_{Mol}$$

$$\Delta G = G_{Mol-Ag_n} - G_{Ag_n} - G_{Mol}$$

where E_s and G_s denote electronic energies and Gibbs free energies of the corresponding *s* species, like benzyl chloride (Mol), Ag_n, and Mol-Ag_n, respectively. For the Gibbs free energy G_s, we considered the correction terms from the thermal energy, entropy, and the zero-point energy (*ZPE*, E_{ZPE}) of vibrations at standard state. The term E_{ZPE} was calculated from the unscaled harmonic vibrational frequencies. As for the adsorption energy, we estimated the bond dissociation energy E_D for benzyl chloride and chlorine molecule. Furthermore, the Gibbs free energy ΔG was used to estimate the equilibrium potential E^0 of the reduction reaction with respect to the standard hydrogen electrode (SHE), which was taken at 4.44 V in an absolute potential scale. Under normal conditions there is a positive potential difference of about 0.241 V between SHE and SCE.

In order to estimate the strength of chemisorption of benzyl species on silver surfaces, we also calculated the Raman spectra of benzyl chloride, adsorbed benzyl chloride and benzyl radical after dissociation on silver based on the corresponding optimized geometries. Raman intensities in Raman scattering processes were estimated in terms of the derivative of the polarizability with respect to a given normal coordinate. In order to obtain the Raman intensities of adsorbates, we employed the classical formula giving Raman intensities under harmonic approximation, where the differential Raman scattering cross section (DRSC) was given by:[31]

$$\left(\frac{d\sigma}{d\Omega}\right)_i = \frac{(2\pi)^4}{45}\cdot\frac{h}{8\pi^2 c\tilde{\nu}_i}\cdot\frac{(\tilde{\nu}_0-\tilde{\nu}_i)^4}{1-\exp(-hc\tilde{\nu}_i/k_BT)}S_i \qquad (1)$$

$$S_i = 45\left(\frac{d\bar{\alpha}}{dQ_i}\right)^2 + 7\left(\frac{d\gamma}{dQ_i}\right)^2 \qquad (2)$$

where σ denotes the Raman scattering cross section per molecule in the solid angle Ω; *h, c*, k_B and *T* have they usual meaning, viz., the Planck constant, light speed, Boltzmann constant, and Kelvin temperature, respectively. The frequencies in cm^{-1} of $\tilde{\nu}_0$ and $\tilde{\nu}_i$ correspond to the incident light and to the *i* th vibrational mode, respectively. In the present calculations, an excitation wavelength at 532 nm was used to simulate Raman spectra. For molecule and adsorbed species, the harmonic vibrational frequencies were calculated, and the obtained frequencies below 2000 cm^{-1} were further scaled by a scaling factor of 0.981 due to the correction of the harmonic approximation and the incomplete properties of theoretical approaches and basis sets.[22, 23] This scaling factor was previously used and validated to scale the vibrational frequencies of pyridine [32],[33], aniline [34], p-aminothiophenol [35], so that calculated results could be precisely matched with the corresponding experimental Raman spectral peaks. S_i in eqn. (2) is the Raman scattering factor (in $Å^4$/amu) that can be directly calculated by Gaussian 09 program. The two terms in Raman scattering activity in equation (2) are derivatives of isotropic and anisotropic polarizabilities with respect to the *i*th normal coordinate, respectively. The polarizability derivatives were obtained by numerically differentiating the analytic polarizability with respect to a given normal mode coordinate.

Finally, based on the surface adsorption configurations and energies calculated by DFT,

we estimated the reaction pathway on the Ag electrode surface and the electron transfer rate constants changes with the cathode potential. Specifically, by taking advantage of the bond dissociative electron transfer theory proposed by Saveant, the rate constant and transfer coefficient were computed to discuss quantitatively the exceptional electrocatalytic effect brought by silver cathodes. [4, 5, 36]

Results and Discussions

1. Adsorption structures and thermodynamic properties of reaction intermediates

The structures of reaction intermediates of benzyl chloride electroreduction were first checked. In the lowest energy configuration of the free benzyl chloride molecule, the C-Cl bond most stable position was found to lie in the plane perpendicular to benzene ring with a C-Cl bond length of 1.841 Å, in good agreement with its experimental measured value of 1.840 Å,[37] *i.e.*, being better than a previously theoretically calculated value of 1.809 Å. [38] Several theoretical papers investigated the dissociative 1-e^- electron transfer of benzyl chloride molecule at inert cathodes,[39-41] considering also the $PhCH_2^{\bullet}$ product obtained after the concerted cleavage of the C-Cl bond,[38] to model the outcome of the first 1e-reduction step at the glassy carbon electrode (Eqns. (3)).[4, 5] In these works, the 1-electron transfer reduction of the benzyl chloride (Eqn. (3)) as well as the ensuing 1-electron transfer (Eqn. (4)) reduction of the benzyl radical were assumed to be outer-sphere electron transfers occurring at the solution side of the Helmholtz layer.

$$PhCH_2Cl + e^- \rightarrow PhCH_2^{\bullet} + Cl^- \qquad E^0_1 \qquad (3)$$

$$PhCH_2^{\bullet} + e^- \rightarrow PhCH_2^- \qquad E^0_2 \qquad (4)$$

According to the theoretical calculation of the change of Gibbs free energy, their standard potential can be calculated from DFT energies.[42] Using 4.44 V for SHE as a reference,[43] we estimated the standard equilibrium potentials at E^0_1 =-0.09 V (Eqn. (3)) and E^0_2 =-1.34 V (Eqn. (4)) vs. SHE, *i.e.* -0.33 V and -1.58 V versus SCE, respectively.

On the other hand, based on DFT investigations of the following reactions,

$$PhCH_2Cl \rightarrow PhCH_2^{\bullet} + Cl^{\bullet} \qquad \mathcal{E}_{D1} \qquad (5)$$

$$Cl_2 \rightarrow 2Cl^{\bullet} \qquad \mathcal{E}_{D2} \qquad (6)$$

$$Cl^{\bullet} + e^- \rightarrow Cl^- \qquad E^0_3 \qquad (7)$$

we could estimate the dissociation energy $\mathcal{E}_{D1}$ of the C-Cl bond in benzyl chloride and that, E_{D2}, of the Cl-Cl bond as well as the standard reduction potential E_3 of chloride ion, *i.e.*, $\mathcal{E}_{D1}$ = 2.94 eV, $\mathcal{E}_{D2}$ = 2.03 eV, and E^0_3 = 2.21 V vs SHE, which were reasonably coherent with the values of 2.99 eV, 2.48 eV, and 2.40 V, respectively, reported in literature.[44] These theoretically calculated results together with previously available results are summarized in Table 1. From these values, the difference between the experimental and theoretical equilibrium potentials noticed above appear to mostly originate from those of the reduction of the chlorine atom.

Table 1. Thermodynamic parameters for standard equilibrium potential (E^0/V vs SHE), bond dissociation energy ($\mathcal{E}_{BDE}$/eV) in gas phase and the PCM model calculated at the UB3LYP/6-311+G** level and some literature data for dissociative reduction of benzyl chloride

Reaction	Gas[a]		PCM[a]		This work		Previous data
	ΔE kcal/mol	ΔG kcal/mol	ΔE^{sol} kcal/mol	ΔG^{sol} kcal/mol	E^0 /V	$\mathcal{E}_{BDE}$ /eV	Expt/Theory /V or eV
Eqn. (3)	-18.96	-33.08	-85.99	-100.27	-0.09		-0.43[b],-0.49[c], -0.52[d],-0.56[e]
Eqn. (4)	-19.23	-22.43	-68.75	-71.58	-1.34		-1.21[e]
Eqn. (5)	66.91	52.38	67.80	53.10		2.94	2.99[d]
Eqn. (6)	47.57	41.61	46.81	40.86		2.03	2.48[f]
Eqn. (7)	-85.87	-85.46	-153.78	-153.37	2.21		1.79[c],2.40[g]

a. Absolute energy obtained by DFT calculations at the UB3LYP/6-311+G** level, in the condition of one atmosphere and the temperature at 298.15K; b. From Ref. [45]; c. From Ref. [42]; d. From Ref. [4]; e. From Ref. [21]; f. From Ref. [43]; g. From Ref. [44].

However, it is expected that electron transfer and C-Cl bond cleavage energies critically depend on interactions with the electrode surface when they are present. This is exactly what our present investigations confirmed. Table 2 summarizes thermodynamic properties, adsorption energies and equilibrium potentials deduced from our DFT calculations. For the adsorption structures of benzyl chloride on the Ag surface, 3 stable adsorption configurations were obtained (*i.e.*, displaying all positive vibrational frequencies) whose optimized geometries are shown in Figure 1c-e. In all these structures, the benzyl chloride attachment involved its chloride that binds to the top surface atom of Ag_{19} clusters, modelling an adsorption at a top site on silver electrodes.

$$PhCH_2Cl + Ag_{19} \rightarrow PhCH_2Cl\text{-}Ag_{19} \qquad \mathcal{E}_{ad1} \qquad (8)$$

The DFT calculated adsorption energies were -2.79, -2.26, and -2.50 kcal/mol, which corresponded to -4.20, -4.10, and -3.98 kcal/mol, respectively, after taking into consideration the solvation effect. It is obvious that the adsorption of benzyl chloride on Ag surfaces is a weakly physical adsorption state. In fact, in the standard state, these Gibbs free energies are all positive with the most stable configuration having a Gibbs free energy of ca. 6.68 kcal/mol. This confirms that the adsorption of benzyl chloride on the Ag surface is thermodynamically unstable but may become important only for kinetic reasons.[21] This clarifies the trend noted in our previous calculations based on a small Ag_4 cluster.[11] Although this adsorption is relatively weak, it has a great influence in accounting the electrocatalytic properties of silver[21] as will be further discussed in the next section.

Considering that benzyl chloride is in a weakly physical adsorption state on the Ag surface, let us expand the mechanism that we proposed in previous works [11, 21] by including a pre-dissociation of the carbon-halogen bond in adsorbed state (Eqn. (9)) followed by reduction of the $PhCH_2$-Ag_{19}-Cl complex into a globally negatively charged assembly without presuming its structure (Eqn. (10)):

$$PhCH_2Cl\text{-}Ag_{19} \rightarrow PhCH_2\text{-}Ag_{19}\text{-}Cl \qquad \mathcal{E}_D \qquad (9)$$

$$PhCH_2\text{-}Ag_{19}\text{-}Cl + e^- \rightarrow PhCH_2\text{-}Ag_{19}\text{-}Cl^- \qquad E^0_4 \qquad (10)$$

Equation (9) is a general formulation encompassing all the processes by which the benzyl chloride adsorbed onto the Ag_{19} cluster (see structures c-e, in Figure 1) directly dissociates into a chlorine atom adsorbed at the three-fold hollow site, and a benzyl radical adsorbed on a top silver site either directly (Figure 1, structures f, g) or through the mediation of the chlorine atom (Figure 1, structure h). Without accounting for the solvation effect, the corresponding average dissociation energy was found to be -19.46 kcal/mol, and the Gibbs free energy -20.89 kcal/mol. When the solvation effect was taken into account, the dissociation energy and the Gibbs free energy were -29.22 kcal/mol and -31.18 kcal/mol, respectively. This clearly evidences that the solvation effect provides an important contribution to drive the dissociation of the adsorbed benzyl chloride. For the chlorine atom adsorbed at the hollow site after dissociation, its Mulliken charges were 0.01 in vacuum and -0.48 for Cl when the solvation effect (PCM model) was taken into account, respectively. When we adopted the natural bond orbital (NBO) method to analyze charge population, its net charge was -0.33 in vacuum and -0.77 in the PCM model. This indicates that the adsorbed chlorine atom was partially reduced into a chloride anion. Meanwhile, the NBO charges of the carbon in the adsorbed benzyl methylene group are -0.51 and -0.69 compared with the Mulliken charges of -0.94 in vacuum and -1.01 in the PCM model. Therefore, the benzyl radical is also adsorbed on the Ag surface in a form close to that of its radical anion while the silver cluster acquired a corresponding positive charge. This is consistent with chemical intuition since the electronegativities of the chlorine atom and of the benzylic radical carbon are obviously larger than that of silver atoms. For example, their Pauling electronegativity values are 3.16, 2.3, and 1.93 for Cl, C, and Ag, respectively. Anyway, compared to the homolytic dissociation of benzyl chloride in Eqn. (5), the electronic structures of the adsorbed moieties in Eqn. (9) are significantly changed. Accordingly, the standard potential of the 1-e reduction in Eqn. (10) was estimated to be about -0.82 V vs SHE, being slightly more negative than the values from the fitting CV analysis[21] and the bond dissociative energy[10, 46].

Since it was reported in literature that chloride ions could not adsorb on the silver surface in the potential range where the benzyl chloride was reduced, we previously suggested that the adsorbed benzyl chloride was reduced into a chloride anion and a benzyl radical adsorbed on the Ag electrode surface after the first electron transfer step. Accordingly, the adsorbed benzyl radical was considered to be further reduced into an adsorbed benzyl anion during the second electron transfer step. To examine this possibility, the standard reduction potentials of adsorbed benzyl radical and chlorine atom were also calculated with the detail according to Eqns. (11 and 12).

$$PhCH_2^{\cdot} + Ag_{19} + e^- \rightarrow PhCH_2Ag_{19}^- \qquad E^0_{2'} \qquad (11)$$

$$Cl^{\cdot} + Ag_{19} + e^- \rightarrow Ag_{19}Cl^- \qquad E^0_{3'} \qquad (12)$$

Table 2. Thermodynamic parameters for standard equilibrium potentials (E^0/V vs SHE), adsorption energies ($\mathcal{E}_{ads}$/eV), bond dissociation energies ($\mathcal{E}_{BDE}$/eV) calculated at the UB3LYP/6-311+G**/LANL2DZ level and partial literature values for dissociative electroreduction of benzyl chloride adsorbed on silver

System	Gas		PCM				Expt/Theory
	ΔE kcal/mol	ΔG kcal/mol	ΔE^{sol} kcal/mol	ΔG^{sol} kcal/mol	E^0 /V	$\mathcal{E}_{ads/BDE}$ /eV	
Eq. (8)	-2.79	5.22	-4.20	6.69		0.29	
Eq. (9)	-19.46	-20.89	-29.22	-31.18		-1.27	
Eq. (10)	-65.51	-65.61	-81.00	-83.43	-0.82		-0.39[b],-0.67[c]
Eq. (11)	-71.85	-58.51	-87.53	-72.57	-1.29		-0.77[b]
Eq. (12)	-130.77	-124.23	-156.39	-125.12	0.99		1.36[d]
Eq. (13)	-17.64	-4.11	-24.60	-10.17		-1.07	
Eq. (14)	-83.93	-73.98	-93.07	-60.68		-4.03	
Eq. (15)	-54.21	-54.40	-62.94	-62.40	-1.73		
Eq. (16)	-46.84	-50.25	-63.32	-64.44	-1.65		

a. The absolute energy obtained by DFT calculations, in the condition of one atmosphere and the temperature at 298.15K. b. From Ref. [21]; c. Estimated from Ref. [10, 46]; d. From Ref. [43].

To estimate the standard reduction potentials $E^0_{2'}$ and $E^0_{3'}$ of the electron transfer for equations (11) and (12), respectively, we calculated separately the adsorption energies of the neutral benzyl radical and chlorine atom (Eqns. (13) and (14) respectively) and the standard reduction potentials $E^0_{2''}$ and $E^0_{3''}$ of their complexes in Eqns. (15, 16) respectively:

$$PhCH_2^{\bullet} + Ag_{19} \rightarrow PhCH_2Ag_{19} \qquad \mathcal{E}_{ad2} \qquad (13)$$

$$Cl^{\bullet} + Ag_{19} \rightarrow Ag_{19}Cl \qquad \mathcal{E}_{ad3} \qquad (14)$$

$$PhCH_2Ag_{19} + e^- \rightarrow PhCH_2Ag_{19}^- \qquad E^0_{2''} \qquad (15)$$

$$Ag_{19}Cl + e^- \rightarrow Ag_{19}Cl^- \qquad E^0_{3''} \qquad (16)$$

The calculated adsorption energy of benzyl radical to Ag_{19} cluster (Eqn. (13)) was -17.64 kcal/mol. In the standard state, its Gibbs free energy of adsorption decreased to -4.11 kcal/mol with an enthalpy equal to -14.53 kcal/mol, which agrees with a significant negative entropy as expected. As illustrated in Table 2, when the solvation effect was taken into account, its adsorption energy and Gibbs free energy becomes drastically more negative, indicating that the solvation effect stabilized the benzyl radical adsorption on the silver surface so as to reach a value akin to those expected for chemical adsorption states. This fully agrees with the above results relative to the charge separations in the product of Eqn. (9) since this confirms its structure having a strongly polar character. In addition, we also noted that upon reducing the benzyl radical into a benzyl anion, the variation of the free energy reached -54.21 kcal/mol, and the solvation energy of the process in which the benzyl anion adsorbed was -28.59

kcal/mol. Based on the relationship between Gibbs free energy and standard potential, we were able to determine a standard reduction potential of adsorbed benzyl radical of ca. -1.73 V vs SHE, or -1.97 V vs SCE which represents a drastic positive shift compared to the reported reduction of benzyl radical at -2.40 V.

The adsorption energy of the chlorine atom on the Ag_{19} surface (Eqn. (14)) was found to be -83.93 kcal/mol, with a Gibbs free energy of -73.98 kcal/mol that became -60.68 kcal/mol after taking into account the solvation effect. The standard reduction potential of the adsorbed chlorine in Eqn. (16), was then evaluated to be -1.65 V vs. SHE. This stresses that the adsorbed chlorine cannot be easily reduced to an anionic state although the chlorine atom has a positive reduction potential.

Figure 2 shows the curves of potential energy surface (PES) along the reaction coordinates for the dissociation of benzyl chloride to benzyl radical and chlorine atom and the desorption of benzyl radical/anion adsorbed on the Ag_{19} cluster. Figure 2a evidences that the C-Cl bond shifts about 2 Å into a dissociative channel state with a very shallow potential well. In Figure 2b, the energy curves were calculated by rigidly scanning the PES along the C-Ag bonds of benzyl radical/anion binding to Ag_{19} cluster. Both PES profiles are almost parallel to each other, indicating that they should have a weakly coupling interaction in dissociative electron transfer. According to the curves of potential energies versus distances between the benzylic carbon center and Ag, it is deduced that the reduction reaction of benzyl radical adsorbed on the Ag surface has to occur in a nonadiabatic process with a very weak coupling in the electron transfer step.

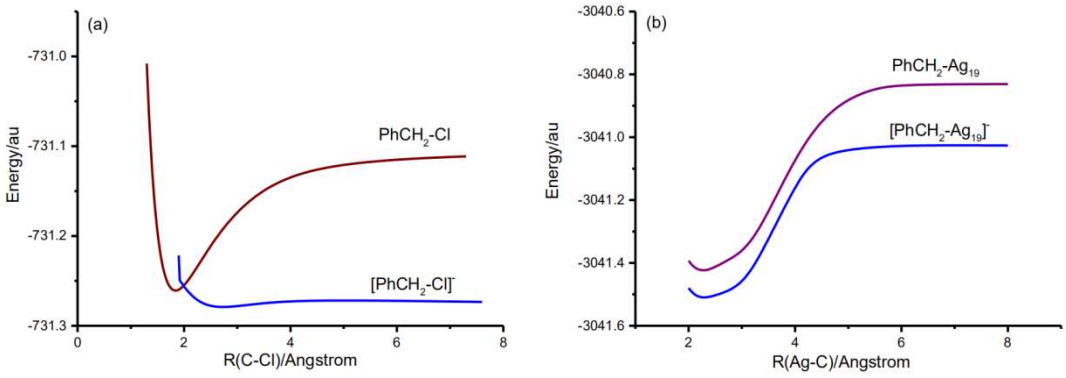

Figure 2. Potential energy curves for free benzyl chloride, benzyl radical and anion intermediates on Ag_{19} cluster. (a) Scanning the PES along the C-Cl bond; (b) Scanning the PES along the Ag-C bonds of benzyl radical and benzyl anion bound to an Ag_{19} cluster.

2. Simulated Raman spectra of reactant and intermediates

The unique property of SERS signals in providing fingerprint information at the molecular level for surface species was extremely important for revealing the electrochemical reduction process of benzyl chloride. In previous work, we have investigated the SERS of the process along which the benzyl radical and its anion were formed. This evidenced that the interaction between the methylene and the silver surface distinctively influenced the relative intensities and the shapes of the SERS peak of the out-of-plane wagging mode.[19, 22, 23]

Let us examine now the calculated Raman spectra of benzyl chloride, adsorbed benzyl

chloride and its dissociative adsorption state with regard to the larger silver cluster (Ag_{19}) considered in this work. The benzyl chloride molecule has 15 atoms with 39 fundamental vibrations which have been identified recently based on a combination of experimental results and theoretical calculations.[22, 37] Figure 3 compares the calculated Raman spectra of benzyl chloride alone in the gas phase (panel a) or in acetonitrile (panel b), or those relative to its undissociated (panel c) or dissociated (panel d) adsorbed intermediates to the experimental Raman spectra (panels e, f) recorded at two different potentials.

The strongest Raman peak at 649 cm^{-1} in Figure 3a corresponds to the stretching vibration of C-Cl bond.[37] It is similar to the observed results by normal Raman spectroscopy and Fourier transform infrared spectroscopy at 690 cm^{-1}, however a precise determination of this vibration frequency is rather difficult. The previous studies adopted hybrid exchange functional B3LYP with different basis sets to calculate, and found that only the three-zeta basis set plus polarization function and diffuse function can afford the correct Raman peak corresponding to the stretching vibration of C-Cl bond. [22, 37, 48] The larger basis sets Aug-cc-pVTZ for C, Cl and H and further 6-311++G(3df,2pd) only for Cl, affords a stretching vibrational frequency of C-Cl bond with a small blue shift to 650 and 654 cm^{-1}, respectively.[22] Three other relatively strong Raman peaks are noticeable in Figure 3a at 997, 1211 and 1610 cm^{-1} featuring the benzene ring breathing, the in-plane C-H bond bending and the C-C bond stretching vibrations, respectively. The wagging vibrational frequency of the methylene group at 1266 cm^{-1} compared well to the calculated value of 1260 cm^{-1} for free benzyl chloride. In addition, it is noted that whereas mono substituted benzenes display strong vibrational peaks in the regions of 690 – 710 cm^{-1} and 730 – 770 cm^{-1}, for benzyl chloride, only relatively weak Raman peaks were observed in these two regions. Examining the solvation effect in acetonitrile (Figure 3b) resulted in a significant increase of the intensity of the Raman peak occurring at 649 cm^{-1} in vacuum (Figure 3a) accompanied by a redshift down to 622 cm^{-1}. Compared to the case of the C-Cl bond vibration, the other calculated frequencies of Raman peaks changed rather slightly between vacuum and solvated benzyl chloride.

Figure 3c presents the calculated Raman spectrum of adsorbed benzyl chloride $PhCH_2Cl$-Ag_{19} clusters before dissociation of the C-Cl bond. Compared to the Raman spectra of the molecule itself (Figure 3a and 3b), the spectral feature and intensity indicate no obvious change in agreement with the rather weak interaction of benzyl chloride with Ag surface as is expected for a physical adsorption. The weak adsorption only causes a slight change of the relative peak intensities. For example, two relatively strong peaks appear at 1208 and 1267 cm^{-1}, corresponding to the in-plane C-H bending vibration of the benzene ring and the wagging of the methylene group, respectively. In this case, the stretching vibration of C-Cl bond slightly shifted to 626 cm^{-1} and became the strongest Raman peak. Figure 3d shows the calculated Raman spectrum after the dissociation of adsorbed benzyl chloride. New and stronger peaks appear at 791 and 816 cm^{-1}. Compared with the calculated Raman spectrum in Figure 3c, the Raman peaks of adsorbed benzyl radical display an intensity about 1000 times stronger than for the undissociated complex. The significant chemical enhancement in Raman intensity may be ascribed to the change from a sp^2 to sp^3 hybridization of the methylene group, the p-π conjugation effect and the strong adsorption interaction between the CH_2 group and silver cluster.[23, 48]

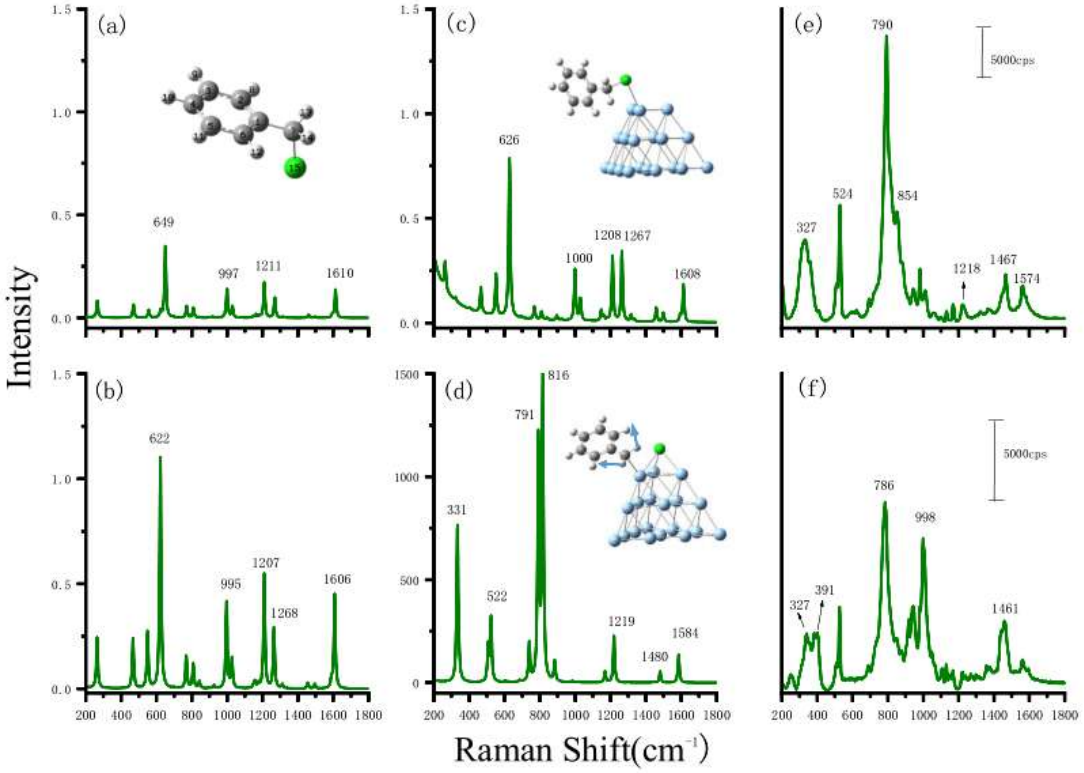

Figure 3. Comparison of calculated and experimental Raman spectra of benzyl chloride under different conditions. The calculated spectra with the absolute intensity unit (10^{-30} cm^2 $mole^{-1}$ sr^{-1}) at the UB3LYP/LANL2DZ(Ag)/6-311+G** level for (a) Benzyl chloride in the gas phase; (b) the solvation of the benzyl chloride in acetonitrile; (c) $PhCH_2Cl$-Ag_{19} cluster; (d) dissociated assembly, *i.e.*, $PhCH_2Cl$-Ag_{19}-Cl^- (note that arrows indicate the normal mode of the CH_2 wagging vibration); (e, f) Experimental SERS spectra recorded at (e) -1.4 V and (f) -1.6 V versus SCE.

The EC-SERS measurement confirmed the presence of two strong overlapping Raman peaks located at around 790 and 854 cm^{-1} respectively in the potential region of -1.4 V as shown in Figure 3e. These strong peaks were assigned to the wagging of the methylene of benzyl species adsorbed on the silver surface.[19] It is noteworthy that the frequency of the vibrational mode significantly redshifted due to the dissociation and the adsorption interaction between the benzyl group and silver surface.[23] When the applied potential was set at -1.6 V, the SERS peak of the wagging modes gradually became weaker and narrower (Figure 3f). The peaks from the adsorbed product observed at 391 and 998 cm^{-1} then became the main features when the potential was further moved to -1.9 V or more (data not shown). The above results also illustrate that EC-SERS signals changed from the weakly adsorbed benzyl chloride to strongly adsorbed benzyl intermediates with high surface concentration. The final product was formed at more negative potentials.

We also investigated the vibrational frequency due to the chloride adsorbed at hollow sites of the silver surface. From our DFT calculations, the symmetrical stretching vibration of three Ag-Cl bonds of a hollow site had a fundamental frequency at 141 cm^{-1} with a Raman

scattering activity being about 175.3 Å^4/amu. This vibrational frequency is lower than that at 240 cm^{-1} for chloride adsorbed at the top site of silver.[49] Moreover we estimated that the absolute Raman intensity for chloride adsorbed at the top site is higher than that at the hollow site. Both factors compare satisfactorily a posteriori with the experimental difficulty of detecting a SERS signal lying in the very low frequency region featuring the chloride ion adsorbed at the hollow site.

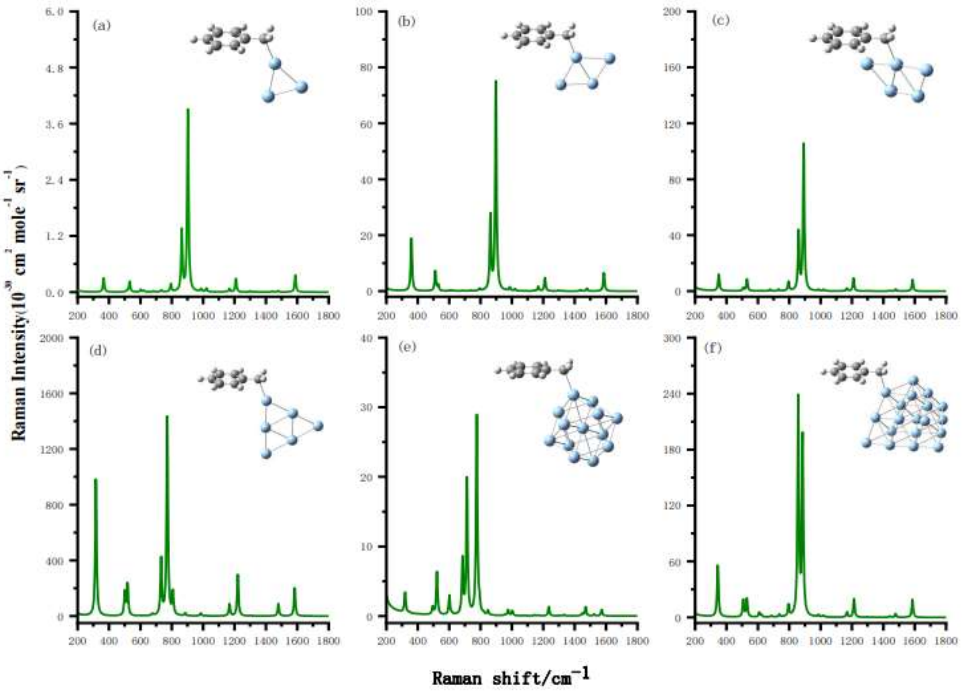

Figure 4. Raman spectra of the [PhCH$_2$-Ag$_n$] neutral complexes predicted for different sizes of silver clusters Ag$_n$ calculated at the UB3LYP/LANL2DZ(Ag)/6-311+G** level. (a) n=3; (b) n=4; (c) n =5; (d) n=6; (e) n=13; (f) n=19.

To evaluate the influence of silver cluster sizes on the SERS spectrum featuring absorbed benzyl moieties on our predictions we calculated the expected Raman spectra for the neutral and negatively charged complexes of the benzyl-Ag$_n$ clusters (n = 3, 4, 5, 6, 13, 19). Figure 4 presents such calculated Raman spectra for a series of [PhCH$_2$-Ag$_n$] neutral complexes. In all these complexes, the benzyl group was found to be adsorbed on top Ag sites through the carbon atom of the methylene group. It is thus not surprising that the wagging vibration of the methylene group had the strongest Raman signals, and that the frequencies and intensities of its signal were dependent on the metal clusters. Except for two clusters (n = 6 and 13) whose peaks of largest intensity were located at 773 and 770 cm^{-1}, the frequencies of the Raman peaks of strongest intensity are those featuring the wagging methylene vibration in the other complexes. For example, PhCH$_2$-Ag$_4$, (Figure 4b) displayed a corresponding peak at 889 cm^{-1} while this occurred at 858 cm^{-1} for PhCH$_2$-Ag$_{19}$ (Figure 4f). For the comparatively weakest Raman peaks, it was found that frequencies and relative intensities changed little with the cluster size, in agreement with the fact that maximum changes for the organic moiety arose from the methylene binding group. The calculated Raman spectra of [PhCH$_2$-Ag$_n$]$^-$ in Figure S1 of the supplementary information also showed that the strong Raman peaks can

again be ascribed to the wagging of CH_2 group of the adsorbed benzyl anion. [19, 22, 23] Nonetheless, these vibrational frequencies remained in the range of 800-880 cm^{-1}, being closely associated with the adsorption interaction of the CH_2 group on the silver surface.

Three overlapping SERS peaks were observed at 790, 854 and 886 cm^{-1} (Figure 3e), corresponding to the CH_2 wagging vibration in weak and strong adsorption states, respectively. [19] This was coherent with the fact that calculated results indicated that the adsorption states of benzyl species on the Ag_{19} surface depended on the surface binding sites chemical activity and applied potentials. As expected, negative potentials favored the reduction of benzyl radical and desorption of its anion, in full agreement with the fact that in EC-SERS spectra recorded at potentials more negative than -1.80 V vs SCE, the Raman peaks related to the intermediate benzyl species disappeared (Figure 3f). [9, 11, 19] This confirmed that the adsorbed benzyl species has desorbed or transformed into products.

3. Synergistic interplay between kinetics and thermodynamics in silver electrocatalysis

The above results indicate that there is effectively a set of interactions between benzyl chloride and the silver cathode surface. However, its initial adsorption is slightly endergonic so it cannot be entirely justifying the strong electrocatalytic effect of silver cathodes. Therefore, as we concluded before, the excellent catalytic effect of silver electrodes on the dissociative reduction of benzyl chloride is necessarily driven by kinetic factors that are allowed by this initial weak adsorption and modify synergistically the overall thermodynamics of the rate determining first electron transfer step.

In a previous contributions of ours[11] we tried to separate the thermodynamic and mechanistic/kinetic contributions by comparing the peak potentials of the irreversible waves featuring the reduction of benzyl chloride at glassy carbon or silver electrodes. That looked perfectly justified because at usual scan rates (<1 V/s) a cathodic peak displaying similar characteristics of irreversible electron transfer with similar transfer coefficient ($\alpha \approx 0.3$) is obtained at each electrode. Their only noticeable difference concerns the drastic positive shift of the wave observed at silver electrode vs. that at glassy carbon.[4, 10, 11, 21] Within this mechanistic framework, we were rightly enticed to consider that the current peak potential value, E^p, of each of these similar irreversible cathodic waves was given by:[50]

$$E^{\mathrm{p}} = E^0 - \frac{RT}{\alpha F}\left[0.78 + \ln\left(\frac{D^{1/2}}{k^0}\right) + \ln\left(\frac{\alpha F \nu}{RT}\right)^{1/2}\right] \qquad (17)$$

where E^0 is the standard potential of the 1-e redox couple controlling thermodynamically the electroreduction reaction and k^0 the corresponding heterogeneous ET rate constant (cm/s) for the cathode material used (ν is the scan rate and D the diffusion coefficient of the reduced substrate; R, F and T have their usual meaning, viz., denote the gas constant, the Faraday constant and the Kelvin temperature, respectively). This allowed to relate the drastic shift of peak potentials observed for a same scan rate upon changing the cathode material to a cumulative change in E^0 and k^0 values:[11]

$$E^p_{\mathrm{Ag}} - E^p_C = \left(E^0_{\mathrm{Ag}} - E^0_C\right) + \frac{RT}{0.3F} ln\left(\frac{k^0_{Ag}}{k^0_C}\right) = 0.5\ V \qquad (18)$$

where $E^p_{\mathrm{Ag}} - E^p_C \approx 0.5\ V$, i.e., for example, $E^p_{\mathrm{Ag}} =$ -1.71 V and $E^p_{\mathrm{C}} =$ -2.21 V vs SCE at 0.2 V/s.[9, 19, 11]

However, the detailed mechanistic analysis performed in ref.[21] that took advantage of the combined use of a wider range of scan rates reaching up to several hundreds of V/s thanks to the use of silver microdisk electrodes, and a thorough analysis of the variations of the CVs based on precise simulations demonstrated that the wave observed at silver cathode could not be described as a classical slow charge transfer irreversible wave (see for example Figure 3 and the corresponding discussion in ref. [21]) as we and all previous authors on the subject did.[9, 19, 11]. In other words, the CV characteristics observed at usual scan rates (v > 1 V/s) during the reduction of benzyl chloride at silver cathodes were only fortuitously looking as those of a classical irreversible electron transfer,[50] hence misleadingly looking as if Equation (17) was obeyed which is not the case. As a consequence, Equation (18) is not valid; accordingly, our former approach[11] results incorrect and cannot be used.

In fact, the single reduction wave of benzyl chloride observed at moderate scan rates at silver cathodes results from a dynamic convolution of two main mechanisms.[21] This convolution could be demonstrated and its mechanistic components resolved only through using high scan rates ($v \geqslant$ 100 V/s). One mechanistic branch, giving rise to a CV component observable at negative potentials (<-2.4V vs. SCE), involves an electron transfer occurring from the electrode to the substrate in solution. This component is identical to that which occurs at glassy carbon electrodes with identical standard potential and heterogeneous rate constant in cm/s of similar order (compare Figure 4Ab in ref. [21]). The second component observable as a pre-wave takes place at less negative potentials (ca. -2.0 V vs. SCE, Figure 5). It features a classical irreversible electron transfer to a benzyl chloride molecule adsorbed onto the silver surface with a rate constant in s^{-1}. This adsorption-controlled component is at the real origin of the electrocatalytic properties of silver cathodes for the reduction of benzyl chloride even if its convolution with the second diffusional-like component hides its role in CV investigations performed at usual scan rates.

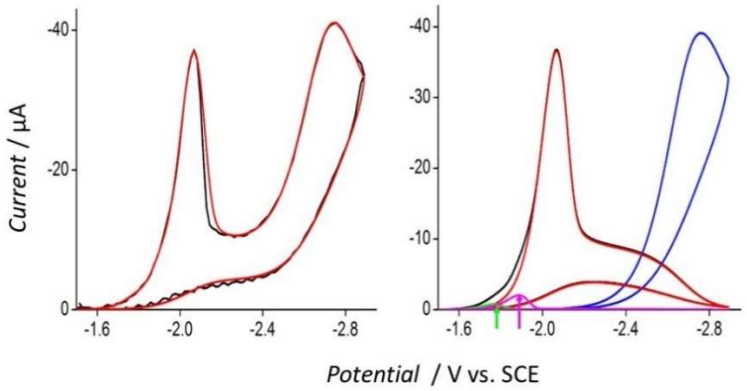

Figure 5. Left: Experimental (black) and best-fit simulated voltammograms (red) of $PhCH_2Cl$ reduction at a 250 µm diameter Ag disk electrode at a scan rates of 500 V/s. Right: Theoretical deconvolution of the CV on the left into its two main components; (blue): diffusion-controlled reduction CV akin to that at a glassy carbon electrode; (black): adsorption-controlled CV with its main wave (red) and its two minor pre-waves marked by green and pink arrows. (*Adapted from Figure 4 ref.* [21]).

For these reasons, if Eqn. (17) was to be used it could apply only to the diffusional

mechanistic branch observed at more cathodic potentials which is identical to that observed at the glassy carbon electrode[5, 36] (same standard potential, same heterogeneous electron transfer rate constant since both depend only on solution and dissolved benzyl chloride properties). Hence, this would have no practical interest. Conversely, the CV wave peak potential, E^{p}_{ads}, of the adsorption-controlled electrocatalytic wave closely follows the classical relationship in Eqn. (19):[50, 51]

$$E^{p}_{ads} = E^{0}_{ads} - \frac{RT}{\alpha_{ads}F}\ln\left(\frac{\alpha F}{RT}\frac{\nu}{k^{0}_{ads}}\right) \qquad (19)$$

that relates E^{0}_{ads}, the standard potential of the 1-e redox couple giving rise to the wave, k^{0}_{ads} the corresponding surface ET rate constant (in s^{-1}), and α_{ads} is the transfer coefficient whose value is obtained from the half-width of the wave $\Delta E_{1/2}$:[50, 51]

$$\alpha_{ads} = 2.44\frac{RT}{F\Delta E_{1/2}} \qquad (20)$$

with $\alpha_{ads} = 0.42$ based on the experimental half-widths determined at several scan rates from 100 to 500 V/s.[21] Note that E^{0}_{ads} = -0.63V vs SCE and $k^{0}_{ads} = 1.1\times10^{-6}\,s^{-1}$ values were reported in ref. [21]. However, this particular set of E^{0}_{ads} and k^{0}_{ads} values was an example selected among many other pairs fitting Eqn. (19) just because it gave the best correlation coefficient between background-corrected experimental and simulated data considering the full voltammograms (see Figure 5, left). However, they should not be firmly relied upon, since several other pairs satisfying equally Eqn. (19) could be obtained depending on the empirical background correction method.

k^{0}_{ads} is relative to an electron transfer to a species adsorbed on a surface, viz., is given by:

$$k^{0}_{ads} = \kappa\times(k_{B}T/h)\times\exp(-\Delta G^{\neq}/k_{B}T) \qquad (21)$$

(where κ is the transmission coefficient, k_B the Boltzmann constant, h the Planck constant, $\Delta G^{\#}$ the activation barrier (in eV) and T is the temperature). Hence, the formalism developed by Saveant et al. to predict $\Delta G^{\#}$ and electron transfer rate constants values from an electrode to species in solution[5, 36, 52] cannot be relied upon in the present context.

For this reason, we investigated by DFT the optimized potential energy surface (PES) intersection along the C-Cl bond distance coordinate presented in Figure 6. This shows that the activation energy barrier in the forward direction is rather small being estimated at ca. 0.2 eV, leading to standard activation free energy $\Delta G^{\#}$ at ca. 0.6 eV. Based on Eqn (21) and assuming a unity value for κ this $\Delta G^{\#}$ value suggests that the maximum rate constant of electron transfer between a silver cathode and an adsorbed benzyl chloride molecule falls in the range of $4.5\text{x}10^{2}\ s^{-1}$. However, this would be a too large value to provide a full irreversible

ET behavior and obeying equations (19, 20) over the whole scan rate range where the absorbed CV wave is observable.[21] Therefore it is presumable that κ is much smaller than unity. Such a conclusion appear to be in full agreement with the extremely acute shape of the local maximum of the potential energy surface in Figure 6. Indeed, such an acute shape suggests that the transition state is close to a conical intersection so that it is presumable that the electron transfer occurs with a transmission coefficient having a value much lower than unity.

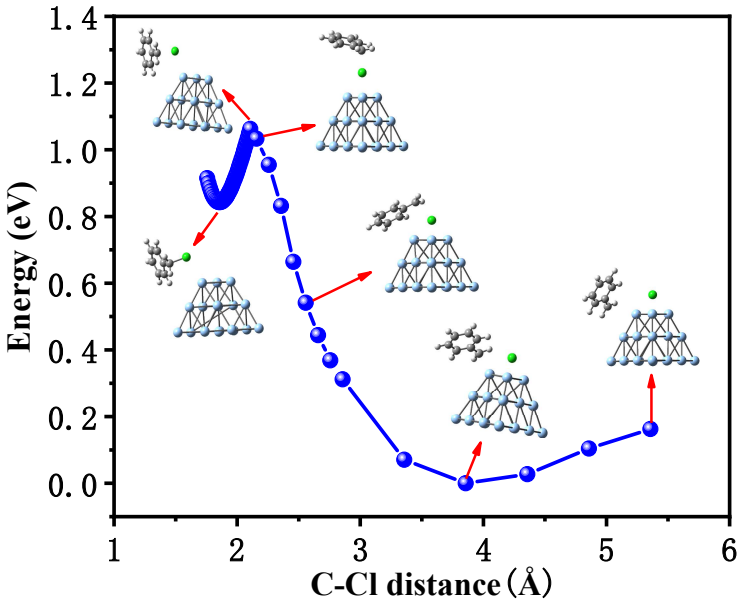

Figure 6. DFT-determined potential energy surface (PES) intersection along the C-Cl bond distance coordinate establishing the dissociative nature of the first reduction step of benzyl chloride adsorbed on a neutral Ag_{19} cluster as calculated at UB3LYP/6-311+G**(C, Cl, and H)/LANL2DZ(Ag) level. The energy is referred to the minimum energy at -3501.70421 au.

In this respect, the DFT results presented in Figure 6 establish that this electron transfer is triply concerted, involving the simultaneous dissociation of the C-Cl bond and the simultaneous chemical adsorptions of the methylene carbon of the benzyl radical through its and of the chloride ion onto the silver surface. Furthermore, the adsorbed benzyl radical and chloride ion pair forms an extended surface complex involving a weak hydrogen bond between one methylene H and the Cl moiety onto the silver surface. The fact that this complex triply-concerted first electron transfer leads to absorbed moieties as established by DFT and SERS analysis above is in full agreement with our previously reported Raman spectral analyses as a function of the electrode potential.[11]

On the one hand, the complexity of this triply concerted electron transfer suggests that only highly specific configurations of the silver-adsorbed benzyl chloride molecules are readily reactive. This observation is in perfect agreement with the fact that the corresponding CV wave involves an overlap of a main wave with two minor pre-waves as is evident in Figure 6. All the above points out to the fact that the corresponding electron transfer occurs with a very small transmission coefficient value.

On the other hand, the potential energy surface describing this first electron transfer evidences that if the weak adsorption of the benzyl chloride onto the silver surface is necessary to allow the electrocatalytic process to occur, its small thermodynamic contribution to the global thermodynamics cannot alone be responsible for the drastic anodic shift (about 0.5 V at typical scan rates) of the benzyl chloride reduction wave at the silver cathodes compared to glassy carbon ones. Conversely, the fact that at the issue of this rate determining first electron transfer step the benzyl radical and chloride ions moieties are highly stabilized by their adsorptions is expected to favors thermodynamically this reaction. In other words, the electrocatalytic performance of silver cathodes founds its origin in a close synergistic coupling between mechanistic (viz. kinetic) and thermodynamic effects.

Owing to the present DFT calculations, both benzyl radical and benzyl anion were strongly adsorbed on silver surface at the end of the first electron transfer step, sharing globally between them a 1e charge. Although the exact mechanisms of their complete reductions and release in solution of the two resulting monoanions are responsible for the ultimate yield of the benzyl chloride 2e-reduction they were not investigated in this work because they occur after the exergonic rate determining triply concerted 1e-transfer and had no significant influence on the overall kinetics. Nonetheless, their reality had already been demonstrated in our previous work[11] by the gradual changes of the EC-SERS spectra observed upon increasing the cathode potential. Indeed, these strongly chemically adsorbed species were observable between -1.2 and -1.8 V vs SCE i.e. as soon as a significant current intensity started to flow, but their EC-SERS signals disappeared at potentials more negative than -1.8 V vs SCE indicating that their reduction into monoanions led to their release in solution.

Conclusion

We systematically investigated the influence of adsorption of reaction intermediates on electrochemical activation of carbon-halogen bonds by combining DFT calculations, surface Raman spectral analysis and bond dissociative electron transfer theory, i.e., to reveal the detailed reaction mechanism of benzyl chloride electrocatalyzed reduction on silver electrodes. The silver surface was described by a sufficiently large silver cluster (Ag_{19}) to offer different possibilities modelling the active site for the reductive cleavage of carbon-chlorine bond for allowing a deep insight of the concerted bond breaking electron transfer process.

DFT results indicated that the benzyl chloride adsorption is rather weak and can be essentially described as a physical one based on its Gibbs free energy. This step is nonetheless crucial to allow the whole mechanism to proceed through a 1-e triply concerted dissociative pathway leading to a benzyl radical and a chlorine, both strongly chemisorbed onto the silver surface and partially charged with a global 1e charge distributed among them. The chlorine moiety is preferentially adsorbed at three-fold hollow sites, resulting in weak Raman signal that remained undetected in previous investigations. Conversely, the EC-SERS signals from adsorbed benzylic intermediates, viz., the benzyl radical and its anion at higher applied potentials, displayed very strong intensities and broad characteristics which could be used to specifically identify and characterize these chemically adsorbed benzylic intermediates on silver electrodes. These SERS peaks mainly feature out-of-plane bending vibration of the methylene group that binds the benzylic moieties to top sites of the silver surface.

By further combining DFT results with previous voltammetric data, we were able to assess the very origin of the electrocatalytic effect of the silver electrode on quantitative bases. As for the high electrocatalytic activity of silver, the strong adsorption of benzyl radical efficiently drives the reduction of the weak benzyl chloride - silver complexes by acting on its thermodynamics, viz., on the standard reduction potential, and on its kinetics, viz., through a decrease of its activation energy. The combination of these two effects causes a positive displacement of more than half a volt of the voltammetric wave at usual scan rates. Its potential position is controlled by the first complex triply concerted electron transfer reaction that is the rate determining step of the overall 2e- reduction process. Preliminary DFT calculations which will be the topic of a further study suggested that the second electron transfer step should be a nonadiabatic reaction.

Overall, the understanding of electrochemical reactions involving weakly physical adsorption reactants and strongly chemical adsorbed intermediates may systematically lead to a high electrocatalytic activity especially when involving synergetic thermodynamics and kinetics roles. This concept may reveal useful for fine understanding of electrocatalytic processes in molecular electrochemistry even when a voltammetric wave does not display any sign of the strong involvement of adsorption steps.

Acknowledgements

The supports from the Chinese Ministry of Science and Technology (2018YFC1602802), the National Natural Science Foundation of China (NSFC) (Nos. 22032004, 21773197, 21703183, 21533006), and Funds of State Key Laboratory of Physical Chemistry of Solid surface and Fujian Science and Technology Office are greatly acknowledged. Y-L.C. thanks the support from the Natural Science Foundation of the Jiangsu Higher Education Institutions of China (20KJB150029), the Open Project of State Key Laboratory of Physical Chemistry of Solid Surfaces (201824). C.A., I.S. and A.O. acknowledge the support from CNRS, ENS - PSL University and Sorbonne University (UMR 8640 PASTEUR). Both Chinese and French teams thank also the Sino-French CNRS IRP NanoBioCatEchem International Laboratory.

References

[1] E.T. Martin, C.M. McGuire, M.S. Mubarak, D.G. Peters, Electroreductive remediation of halogenated environmental pollutants, Chemical Reviews, 116 (2016) 15198-15234.

[2] M.S. Mubarak, D.G. Peters, Using silver cathodes for organic electrosynthesis and mechanistic studies, Current Opinion in Electrochemistry, 2 (2017) 60-66.

[3] J.-M. Saveant, Molecular catalysis of electrochemical reactions. Mechanistic aspects, Chemical Reviews, 108 (2008) 2348-2378.

[4] C.P. Andrieux, A. Legorande, J.M. Saveant, Electron-transfer and bond breaking - examples of passage from a sequential to a concerted mechanism in the electrochemical reductive cleavage of arylmethyl halides, Journal of the American Chemical Society, 114 (1992) 6892-6904.

[5] J.M. Saveant, A simple-model for the kinetics of dissociative electron-transfer in polar-solvents - application to the homogeneous and heterogeneous reduction of alkyl-halides, Journal of the American Chemical Society, 109 (1987) 6788-6795.

[6] J.M. Saveant, Dissociative electron-transfer - new tests of the theory in the electrochemical and homogeneous reduction of alkyl-halides, Journal of the American Chemical Society, 114 (1992)

10595-10602.
[7] S. Rondinini, P.R. Mussini, P. Muttini, G. Sello, Silver as a powerful electrocatalyst for organic halide reduction: the critical role of molecular structure, Electrochimica Acta, 46 (2001) 3245-3258.
[8] M. Fedurco, C.J. Sartoretti, J. Augustynski, Reductive cleavage of the carbon-halogen bond in simple methyl and methylene halides. Reactions of the methyl radical and carbene at the polarized electrode/aqueous solution interface, Langmuir, 17 (2001) 2380-2387.
[9] A.A. Isse, S. Gottardello, C. Durante, A. Gennaro, Dissociative electron transfer to organic chlorides: Electrocatalysis at metal cathodes, Physical Chemistry Chemical Physics, 10 (2008) 2409-2416.
[10] A.A. Isse, P.R. Mussini, A. Gennaro, new insights into electrocatalysis and dissociative electron transfer mechanisms: The case of aromatic bromides, Journal of Physical Chemistry C, 113 (2009) 14983-14992.
[11] Y.F. Huang, D.Y. Wu, A. Wang, B. Ren, S. Rondinini, Z.Q. Tian, C. Amatore, Bridging the gap between electrochemical and organometallic activation: Benzyl chloride reduction at silver cathodes, J Am Chem Soc, 132 (2010) 17199-17210.
[12] A.A. Isse, A. De Giusti, A. Gennaro, L. Falciola, P.R. Mussini, Electrochemical reduction of benzyl halides at a silver electrode, Electrochimica Acta, 51 (2006) 4956-4964.
[13] S. Ardizzone, G. Cappelletti, P.R. Mussini, S. Rondinini, L.M. Doubova, Adsorption competition effects in the electrocatalytic reduction of organic halides on silver, J Electroanal Chem, 532 (2002) 285-293.
[14] M. Fedurco, L. Coppex, J. Augustynski, Ab initio and electrochemical studies on the reductive bond dissociation in haloethanols, J Phys Chem B, 106 (2002) 2625-2633.
[15] S. Arnaboldi, A. Gennaro, A.A. Isse, P.R. Mussini, The solvent effect on the electrocatalytic cleavage of carbon-halogen bonds on Ag and Au, Electrochim Acta, 158 (2015) 427-436.
[16] D.-Y. Wu, J.-F. Li, B. Ren, Z.-Q. Tian, Electrochemical surface-enhanced Raman spectroscopy of nanostructures, Chemical Society Reviews, 37 (2008) 1025-1041.
[17] D.-Y. Wu, M. Zhang, L.-B. Zhao, Y.-F. Huang, B. Ren, Z.-Q. Tian, Surface plasmon-enhanced photochemical reactions on noble metal nanostructures, Science China-Chemistry, 58 (2015) 574-585.
[18] C. Zhan, X.-J. Chen, Y.-F. Huang, D.-Y. Wu, Z.-Q. Tian, Plasmon-mediated chemical reactions on nanostructures unveiled by surface-enhanced Raman spectroscopy, Accounts of Chemical Research, 52 (2019) 2784-2792.
[19] A. Wang, Y.F. Huang, U.K. Sur, D.Y. Wu, B. Ren, S. Rondinini, C. Amatore, Z.Q. Tian, In Situ Identification of Intermediates of benzyl chloride reduction at a silver electrode by sers coupled with dft calculations, J Am Chem Soc, 132 (2010) 9534-9536.
[20] O.V. Klymenko, I. Svir, C. Amatore, New theoretical insights into the competitive roles of electron transfers involving adsorbed and homogeneous phases, Journal of Electroanalytical Chemistry, 688 (2013) 320-327.
[21] O.V. Klymenko, O. Buriez, E. Labbe, D.-P. Zhan, S. Rondinini, Z.-Q. Tian, I. Svir, C. Amatore, Uncovering the missing link between molecular electrochemistry and electrocatalysis: Mechanism of the reduction of benzyl chloride at silver cathodes, ChemElectroChem, 1 (2014) 227-240.
[22] Y.-L. Chen, R. Panneerselvam, D.-Y. Wu, Z.-Q. Tian, Theoretical study of normal Raman spectra and SERS of benzyl chloride and benzyl radical on silver electrodes, Journal of Raman Spectroscopy, 48 (2017) 53-63.

[23] S. Tao, L.-J. Yu, R. Pang, Y.-F. Huang, D.-Y. Wu, Z.-Q. Tian, Binding interaction and Raman spectra of p-π conjugated molecules containing CH_2/NH_2 groups adsorbed on silver surfaces: A dft study of wagging modes, J Phys Chem C, 117 (2013) 18891-18903.
[24] A.A. Isse, S. Gottardello, C. Maccato, A. Gennaro, Silver nanoparticles deposited on glassy carbon. Electrocatalytic activity for reduction of benzyl chloride, Electrochem Commun, 8 (2006) 1707-1712.
[25] J. Tomasi, B. Mennucci, R. Cammi, Quantum mechanical continuum solvation models, Chemical Reviews, 105 (2005) 2999.
[26] G.W.T. M. J. Frisch, H. B. Schlegel, G. E. Scuseria,, J.R.C. M. A. Robb, G. Scalmani, V. Barone, B. Mennucci,, H.N. G. A. Petersson, M. Caricato, X. Li, H. P. Hratchian,, J.B. A. F. Izmaylov, G. Zheng, J. L. Sonnenberg, M. Hada,, K.T. M. Ehara, R. Fukuda, J. Hasegawa, M. Ishida, T. Nakajima,, O.K. Y. Honda, H. Nakai, T. Vreven, J. A. Montgomery, Jr.,, F.O. J. E. Peralta, M. Bearpark, J. J. Heyd, E. Brothers,, V.N.S. K. N. Kudin, T. Keith, R. Kobayashi, J. Normand,, A.R. K. Raghavachari, J. C. Burant, S. S. Iyengar, J. Tomasi,, N.R. M. Cossi, J. M. Millam, M. Klene, J. E. Knox, J. B. Cross,, C.A. V. Bakken, J. Jaramillo, R. Gomperts, R. E. Stratmann,, A.J.A. O. Yazyev, R. Cammi, C. Pomelli, J. W. Ochterski,, K.M. R. L. Martin, V. G. Zakrzewski, G. A. Voth,, J.J.D. P. Salvador, S. Dapprich, A. D. Daniels,, J.B.F. O. Farkas, J. V. Ortiz, J. Cioslowski,, and D. J. Fox, Gaussian 09,, Gaussian, Inc., 2013.
[27] K. Raghavachari, Binkley, J. S., Seeger, R. and Pople, J. A., Self-Consistent Molecular Orbital Methods. 20. Basis set for correlated wave-functions, J Chem Phys, 72 (1980) 650.
[28] T.H.Dunning Jr., Gaussian basis sets for use in correlated molecular calculations. I. The atoms boron through neon and hydrogen, Journal of Chemical. Physics, 90 (1989) 1007.
[29] P.J. Hay, W.R. Wadt, Ab initio effective core potentials for molecular calculations – potentials for the transition-metal atoms Sc to Hg, J Chem Phys, 82 (1985) 270.
[30] J.B. Foresman, A.E. Frisch, Exploring Chemistry with Electronic Structure Methods, Gaussian, Inc.1998.
[31] B.S. Galabov, T. Dudev, Vibrational Spectra and Structure. Vol. 22 Vibrational Intensities, Elsevier, Amsterdam, 1996.
[32] D.Y. Wu, B. Ren, Y.X. Jiang, X. Xu, Z.Q. Tian, Density functional study and normal-mode analysis of the bindings and vibrational frequency shifts of the pyridine-M (M = Cu, Ag, Au, Cu+, Ag+, Au+, and Pt) complexes, J Phys Chem A, 106 (2002) 9042-9052.
[33] D.-Y. Wu, X.-M. Liu, S. Duan, X. Xu, B. Ren, S.-H. Lin, Z.-Q. Tian, Chemical enhancement effects in SERS spectra: A quantum chemical study of pyridine interacting with copper, silver, gold and platinum metals, J Phys Chem C, 112 (2008) 4195-4204.
[34] L.-B. Zhao, R. Huang, M.-X. Bai, D.-Y. Wu, Z.-Q. Tian, Effect of aromatic amine-metal interaction on surface vibrational raman spectroscopy of adsorbed molecules investigated by density functional theory, J Phys Chem C, 115 (2011) 4174-4183.
[35] D.-Y. Wu, X.-M. Liu, Y.-F. Huang, B. Ren, X. Xu, Z.-Q. Tian, Surface catalytic coupling reaction of p-mercaptoaniline linking to silver nanostructures responsible for abnormal sers enhancement: A DFT study, J Phys Chem C, 113 (2009) 18212-18222.
[36] L. Pause, M. Robert, J.M. Saveant, Reductive cleavage of carbon tetrachloride in a polar solvent. An example of a dissociative electron transfer with significant attractive interaction between the caged product fragments, Journal of the American Chemical Society, 122 (2000) 9829-9835.
[37] P.B. Nagabalasubramanian, S. Periandy, S. Mohan, Ab initio HF and DFT simulations, FT-IR and FT-Raman vibrational analysis of alpha-chlorotoluene, Spectrochimica Acta Part a-Molecular

and Biomolecular Spectroscopy, 77 (2010) 150-159.
[38] R. Benassi, C. Bertarini, F. Taddei, The dissociative nature of the radical anion of benzyl chloride. A theoretical MO ab initio approach, Chem Phys Lett, 257 (1996) 633-638.
[39] C. Fontanesi, P. Baraldi, M. Marcaccio, On the dissociation dynamics of the benzyl chloride radical anion. An ab initio dynamic reaction coordinate analysis study, J Mol Struc-Theochem, 548 (2001) 13-20.
[40] R. Benassi, C. Bertarini, F. Taddei, Theoretical MO ab initio investigation of the reductive C-Cl bond cleavage in benzyl chloride, benzotrichloride and in the analogous 4-pyridine derivatives, Journal of the Chemical Society-Perkin Transactions 2, (1997) 2263-2269.
[41] P.I. Dem'yanov, E.M. Myshakin, G. Boche, V.S. Petrosyan, L.N. Alekseiko, Ab initio MO and density functional theory study of substituent effects on electron attachment to benzyl chlorides, J Phys Chem A, 103 (1999) 11469-11473.
[42] A.A. Isse, C.Y. Lin, M.L. Coote, A. Gennaro, Estimation of Standard Reduction Potentials of Halogen Atoms and Alkyl Halides, Journal of Physical Chemistry B, 115 (2011) 678-684.
[43] M.T.M. Koper, G.A. Voth, A three-dimensional potential energy surface for dissociative adsorption and associative desorption at metal electrodes, Journal of Chemical Physics, 109 (1998) 1991-2001.
[44] M.L. Alegre, M. Gerones, J.A. Rosso, S.G. Bertolotti, A.M. Braun, D.O. Martire, M.C. Gonzalez, Kinetic study of the reactions of chlorine atoms and Cl-2(center dot-) radical anions in aqueous solutions. 1. Reaction with benzene, Journal of Physical Chemistry A, 104 (2000) 3117-3125.
[45] C.Y. Lin, M.L. Coote, A. Gennaro, K. Matyjaszewski, Ab initio evaluation of the thermodynamic and electrochemical properties of alkyl halides and radicals and their mechanistic implications for atom transfer radical polymerization, Journal of the American Chemical Society, 130 (2008) 12762-12774.
[46] A.A. Isse, L. Falciola, P.R. Mussini, A. Gennaro, Relevance of electron transfer mechanism in electrocatalysis: the reduction of organic halides at silver electrodes, Chemical Communications, 42 (2006) 344-346.
[47] Z.Y. Zhou, H.W. Gao, L. Guo, Y.H. Qu, X.L. Cheng, Analysis of vibrational spectra of chlorotoluene based on density function theory calculations, Spectrochim Acta A, 58 (2002) 1553-1558.
[48] S. Tao, L.-J. Yu, D.-Y. Wu, Z.-Q. Tian, Raman spectra of amino wagging vibrational modes in p-π-conjugated molecules, Acta Physico-Chimica Sinica, 29 (2013) 1609-1617.
[49] R. Pang, X.-G. Zhang, J.-Z. Zhou, D.-Y. Wu, Z.-Q. Tian, SERS chemical enhancement of water molecules from halide ion coadsorption and photoinduced charge transfer on silver electrodes, J Phys Chem C, 121 (2017) 10445-10454.
[50] A.J. Bard, L.R. Faulkner, Electrochemical Methods. Fundamentals and Applications, 2rd Edition ed., John Wiley & Sons, Inc., New York, 2001.
[51] E. Laviron, General expression of the linear potential sweep voltammogram in the case of diffusionless electrochemical systems, J. Electroanal. Chem., 101 (1979) 19-28.
[52] A.A. Isse, L. Scarpa, C. Durante, A. Gennaro, Reductive cleavage of carbon-chlorine bonds at catalytic and non-catalytic electrodes in 1-butyl-3-methylimidazolium tetrafluoroborate, Phys Chem Chem Phys, 17 (2015) 31228-31236.